D4°

N79-24041

SCALING LAWS AND EDGE EFFECTS FOR POLYMER SURFACE DISCHARGES*

Keith G. Balmain
University of Toronto

SUMMARY

Specimens of Mylar sheet were exposed to a 20 kV electron beam. The resulting surface discharge arcs were photographed and the discharge current into a metal backing plate measured as a function of time. The area of the Mylar sheet was defined by a round aperture in a close-fitting metal mask, and the current pulse characteristics were plotted against area on log-log paper. The plots appear as straight lines (due to power-law behavior) with slopes of 0.50 for the peak current, 1.00 for the charge released, 1.49 for the energy and 0.55 for the pulse duration. In addition, evidence is presented for the occurrence of banded charge distributions near grounded edges, on both Teflon and Mylar.

INTRODUCTION

Numerous extensive laboratory simulation studies on spacecraft dielectric charging and arc discharging have been reported in references 1, 2 and 3. Many such laboratory experiments involved dielectric areas much smaller than the exposed dielectric areas existing on operational synchronous-orbit satellites, and so the question of area scaling of charge/discharge phenomena arises naturally. Certainly it is easier and faster to carry out small-scale experiments, compared to large-scale experiments in vacuum chambers large enough to hold spacecraft components or even an entire spacecraft.

Experimental results reported in reference 4 showed that, for surface macrodischarges on metal-backed polymer dielectrics, the peak discharge current is proportional to the surface area raised to a power "p" lying between 0.5 and 0.8, for the range of areas lying between 0.2 cm^2 and 20 cm^2. The most consistent results were for Teflon with a value p = 0.575, giving a peak-current power law which extrapolated downward in area into close proximity with microdischarge measurements in the range of areas from 10^{-5} cm^2 to $10^{-3} cm^2$.

The above extrapolation would have produced a better fit if the value of p had been slightly lower. This observation raises the question of area definition, because in the macrodischarge case the charged area was defined by

*Research supported by the Natural Sciences and Engineering Research Council of Canada under Grant No. A-4140. The measurements reported here were carried out primarily by G.R. Dubois.

cutting the specimen to size, while in the microdischarge case the charged area was defined by the cross-sectional area of the incident electron beam as deduced from scanning-electron-microscope examination of deposited charge patterns. For the macrodischarges, cutting the specimen to size could stress or otherwise damage the specimen edge, and furthermore leaving this edge exposed could produce anomalous effects on charge penetration, charge accumulation, discharge initiation and discharge propagation.

A method of area definition which is precise and which does not involve cutting or edge exposure is to cover the specimen with a close-fitting metal mask and to use masks with various apertures in order to establish experimentally the area scaling laws. This paper describes such a masking technique and gives experimental results of discharge characteristics obtained using masked Mylar specimens.

If a metal mask avoids some types of edge effects, it is reasonable to wonder what edge effects remain. One type of masked-dielectric edge effect was noted by M. Cuchanski and first reported in reference 5. It involved exposure to an electron beam of a polymer sheet covered by a vacuum-deposited-aluminum mask with a circular aperture. This was followed first by exposure to air to neutralize surface charge and then by examination in a scanning electron microscope at low voltage to look for embedded charge made visible by its enhancement of secondary emission. Charged annular rings were observed, suggesting the existence of high-field regions near the mask edge. This work was later extended (ref. 6) and some of these latter results are included here.

EXPERIMENTAL ARRANGEMENT

The masked specimen and its backing plate are shown in figure 1 and are mounted on (and isolated from) a removable section of the vacuum chamber wall. A vacuum-sealed bulkhead receptacle carries the discharge pulse signal through the chamber wall to a 10-ohm termination and thence via attenuators to a 400-MHz oscilloscope.

The incident electron beam is deflected magnetically in order to permit photography of the surface arc discharge. The resultant current density at the specimen surface is of the order of 1 $\mu A/cm^2$ at a beam accelerating voltage of 20 kV. Precautions had to be taken to ensure adequate shielding of operating personnel from X-radiation.

A different Mylar specimen cut from the same sheet was used for each masked area to produce the results presented graphically in this paper.

DISCHARGE MEASUREMENTS

A typical photograph of a surface arc on Mylar is shown in figure 2. The arc concentration at several points around the mask edge is evident and is common to all arcs photographed. Also visible in most photographs (although

not strongly evident in this case) is the alignment of many of the interior arcs along a preferred direction dependent on specimen orientation.

Typical discharge current pulses are shown in figure 3. For smaller areas the pulses were more sharply peaked, and for the smallest areas tested the pulses were much shorter with some overshoot and ringing noticeable.

The variation of peak current I_m with specimen area is shown in figure 4, in which each point is the average from approximately ten pulses. The straight line drawn through the points has a slope of 0.50 indicating that the peak current is proportional to the area raised to the power 0.50. It is worth noting that this line extrapolates to I_m = 1000 A at an area of 1 m^2.

The charge Q passing through the measurement system is given by

$$Q = \int I \, dt$$

and this integration was carried out manually from oscilloscope photographs. The resulting graph of charge against area is shown in figure 5, in which each point is the average from approximately five pulses. The straight-line approximation has a slope of 1.00 and the fit to the straight line is good even for small areas.

The energy dissipated in the load resistor R is given by

$$E = R \int I^2 \, dt$$

The resulting graph of energy against area is shown in figure 6, in which each point is the average from approximately five pulses. The straight-line approximation has a slope of 1.49. It should be noted that the highest energies are of the order of a few millijoules, indicating that unsuitable load resistors or attenuators attached to the system could be burned out by the discharge pulses.

The pulse duration was calculated from the relation

$$T = \frac{1}{I_m} \int I \, dt$$

The resulting graph of duration against area is shown in figure 7. The points exhibit more scatter than in the other graphs, with the result that the straight-line approximation having a slope of 0.55 could almost as well have been drawn with slopes anywhere in the range from 0.50 to 0.58. Departure from the straight-line approximation is most noticeable for small areas and thus for short pulses, this departure taking the form of lowered amplitudes and extended pulse durations, accompanied by small-amplitude ringing for the smallest areas. The probable primary cause of this effect is the 400 MHz bandwidth of the oscilloscope, with a secondary cause being the overall dimensions of the specimen, mask, back-plate and distance to the load, all adding up to about a wavelength at 1000 MHz.

The penetration depth for 20 kV electrons in Mylar is estimated to be 8 μm (ref. 6), so presumably most of the embedded charge resides near this depth. If discharge arc propagation and subsequent damage are concentrated near the penetration depth as in the high-energy experiments of Gross (ref. 7),

then one might expect to see surface damage of about 8 μm depth. A Mylar specimen which had been used for many experiments was coated with vacuum-deposited gold and viewed in a scanning electron microscope, a typical result being shown in figure 8. The large depression is about 8 μm deep and presumably resulted from the blowoff of material during the propagation of an arc along the groove at the bottom of the depression. The groove has branches which seem to disappear into holes in the depression wall. The corresponding transmitted-light photograph of figure 9 indicates that the holes continue into the material, forming a network of damage tracks or tunnels of about 2 μm diameter at a depth of about 8 μm.

The propagation of a discharge along a well-defined path must of course take place at an equally well-defined velocity. This velocity can be estimated by noting from figure 7 that an aperture radius of 1 cm corresponds to a pulse duration of 33 ns, the ratio giving a velocity of 3×10^5 m/s. This is similar to the value of roughly 10^5 m/s which can be deduced by means of the same type of calculation from the results in references 5 and 6 for microdischarges.

The banded charge distributions near a metallization edge (as referred to in the Introduction) are shown in figure 10. The basic procedure used was first to irradiate the exposed dielectric in the aperture with a scanned 20 kV electron beam while viewing the secondary-electron image, in the usual scanning electron microscope (SEM) set-up. Then the specimen was exposed briefly to room air to neutralize most of the surface charge. The specimen was then returned to the SEM, scanned at 1 kV and its secondary-electron image photographed. Because embedded charge must increase secondary emission due to electrostatic repulsion, the area of embedded negative charge shows up as a lighter region in the photographs. In figure 10, the top row of photographs shows the annular-ring form of the charged bands on both Teflon and Mylar. In the middle row a discharge event is indicated by the white streak, which appears to have caused an indentation in the charged band. Perhaps the discharge was initiated in the charged band near the metallization edge. In the bottom row, notch-shaped and rectangular apertures were tried with similar results.

INTERPRETATION

The area-scaling graphs of I_m, Q and T are all approximately consistent with the notion of a discharge arc which propagates at a well-defined velocity. If the discharge originated from a point and expanded outward uniformly, then the current would be proportional to the length of the wavefront, and l_m would be proportional to its maximum length, a quantity related in turn to the linear dimensions of the specimen. A sequence of linear, branching discharge paths should produce the same result.

If the discharge initiates at the aperture edge and propagates inward, the replacement current into the metal base could arise in two ways. One way is for electrons to be ejected at or near the arc wavefront. The other is for the electrons to be propelled down the network of damage tunnels to the point of initiation where they are ejected, there giving rise to the replacement

current. In the latter case the relevant velocity would be the sum of the arc velocity and the electron expulsion velocity along the tunnels.

A vivid analogy is that of a "flash flood" caused by a rainstorm of specified area. If the water runoff velocity were constant then the peak runoff current flow would be proportional to the square root of the storm area.

Clearly the surface discharge is not at all similar to a capacitor discharge. Although the capacitor released charge is proportional to the capacitor plate area (as in fig. 5), its peak discharge current is also proportional to the plate area (in contrast to fig. 4).

CONCLUSIONS

Surface discharge arcs on metal-backed Mylar (and probably on a wide range of polymers) exhibit characteristics which scale with variations in specimen area according to very well defined power laws. The characteristics identified are peak current, released charge, released energy and pulse duration, and the respective powers are 0.50, 1.00, 1.49 and 0.55. The latter figure of 0.55 for pulse duration probably would become 0.50 with improved experimental technique, because it is determined pulse-by-pulse as the ratio of released charge to peak current. For small areas and thus for short pulses, departures from power-law behaviour are believed due to limited oscilloscope bandwidth.

The discharge arcs appear to propagate at about 3×10^5 m/s in hair-like, branching tunnels at the penetration depth, with occasional blowoffs of surface material. Probably these discharge tunnels are not re-used by subsequent discharges, because the appearance of discharge arcs always changes markedly from one arc to the next.

Specimen edges play a special role, with cut and exposed edges significantly affecting the area scaling laws. Charge accumulates with greatest density near an edge, usually in multiple bands parallel to the edge. Indications are that these charged bands offer preferential sites for discharge initiation.

REFERENCES

1. Rosen, A. (Ed.): Spacecraft Charging by Magnetospheric Plasmas. Progress in Astronautics and Aeronautics, vol. 47, 1976. (Pub. by AIAA and MIT Press).

2. Pike, C.P.; Lovell, R.R. (Eds.): Proceedings of the Spacecraft Charging Technology Conference. Report AFGL-TR-77-0051/NASA TMX-73537, 24 Feb. 1977.

3. Proceedings of the 1978 Symposium on the Effect of the Ionosphere on Space and Terrestrial Systems, Washington DC, sponsored by NRL/ONR.

4. Balmain, K.G.; Kremer, P.C.; Cuchanski, M.: Charged-Area Effects on Spacecraft Dielectric Arc Discharges. In reference 3.

5. Balmain, K.G.: Charge/Discharge and Electromagnetic Radiation Studies on Spacecraft Materials and Structures. Final report on DSS Contract No. OSU76-00064 prepared for the Department of Communications, Canada, April 1977.

6. Cuchanski, M.: Simulation Studies of Charging, Discharging and Discharge Pulse Propagation on Spacecraft Materials and Structures. M.A.Sc. Thesis, Department of Elect. Engrg., University of Toronto, 1978.

7. Gross, B.: Irradiation Effects in Plexiglas. J. Polymer Sci., vol. 27, 1958, pp. 135-143.

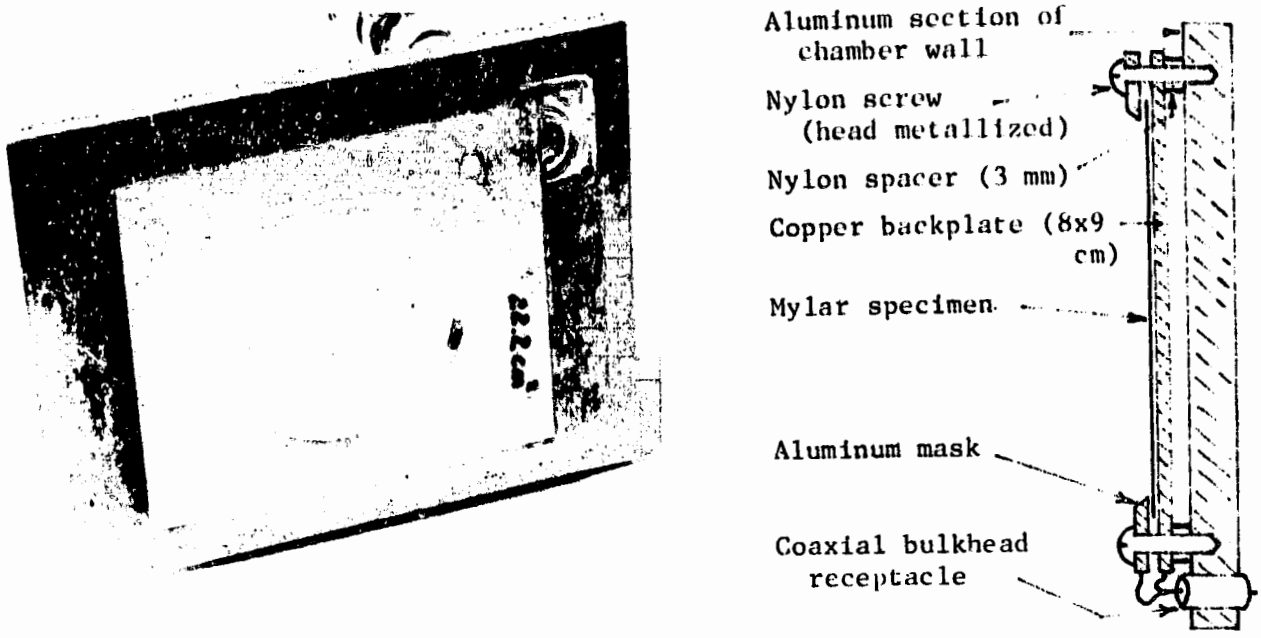

Figure 1. The specimen mounting assembly with circular-aperture aluminum mask. The specimens used in the experiments were Mylar sheets 120 μm thick.

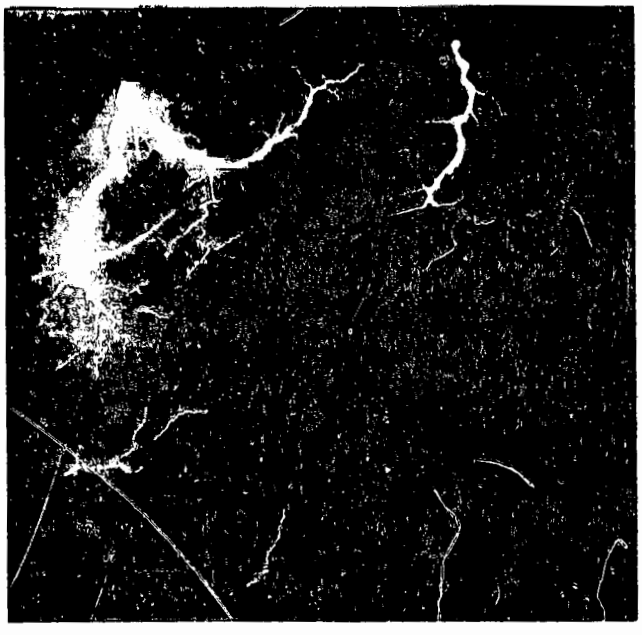

Figure 2. A typical arc discharge on a 47.6 cm^2 Mylar specimen.

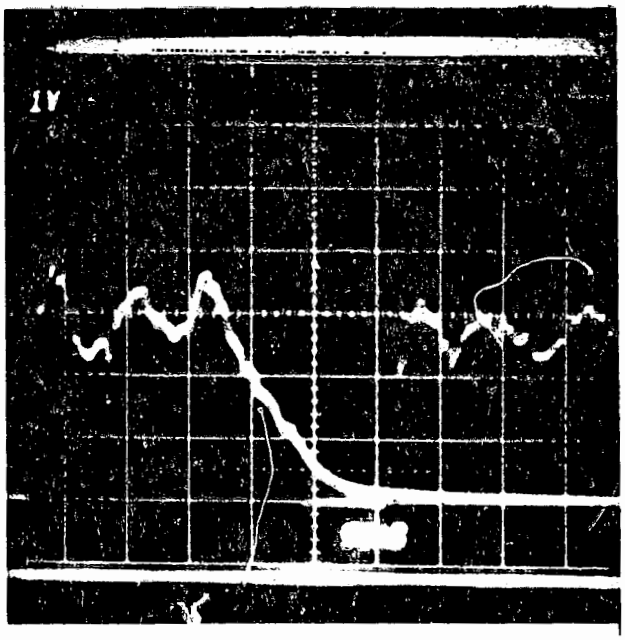

Figure 3. Two typical current pulses from a 22.2 cm^2 Mylar specimen. I_m=30.2A and 26.2A

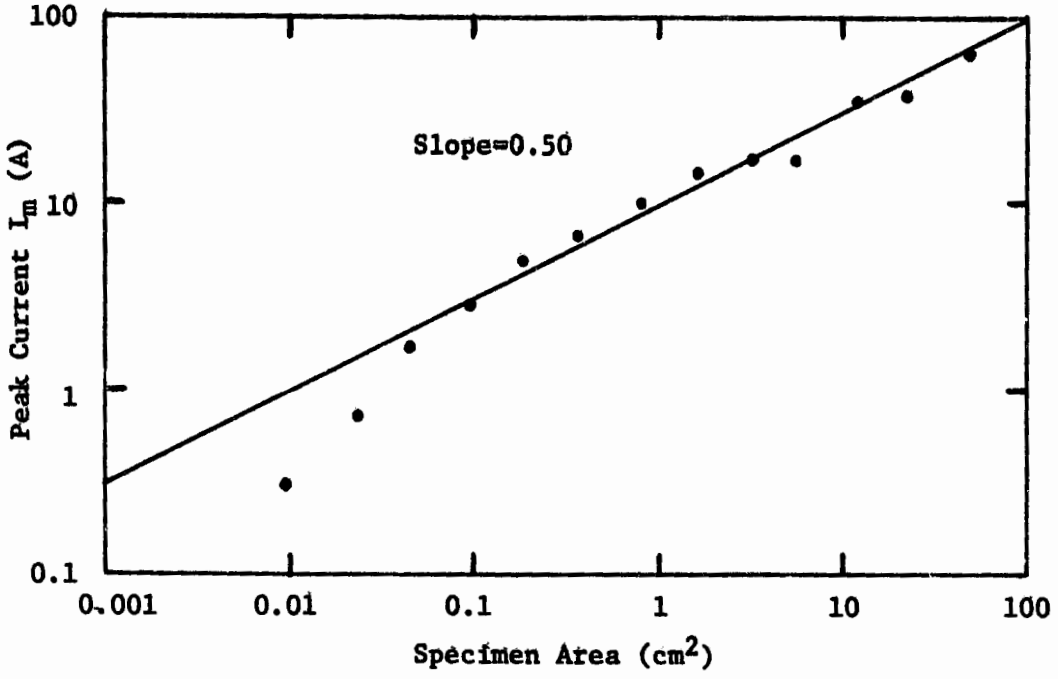

Figure 4. The variation of peak current I_m with Mylar specimen area.

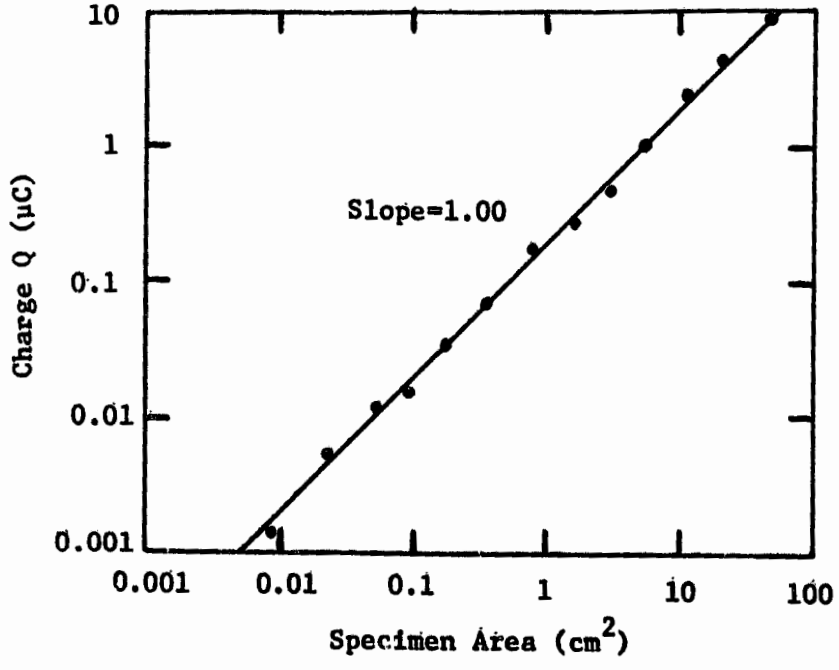

Figure 5. The variation of released charge $Q = \int I\,dt$ with Mylar specimen area.

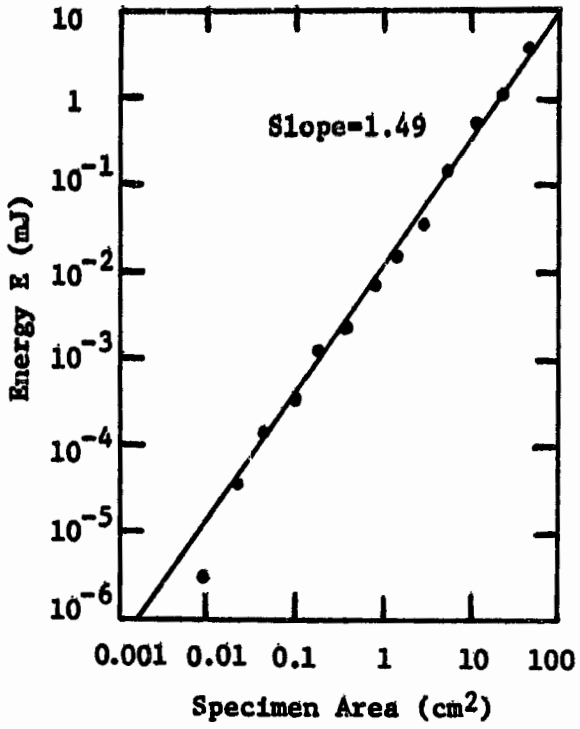

Figure 6. The variation of energy $E = R \int I^2 \, dt$ with Mylar specimen area. The energy is dissipated in a load resistor R=10 ohms.

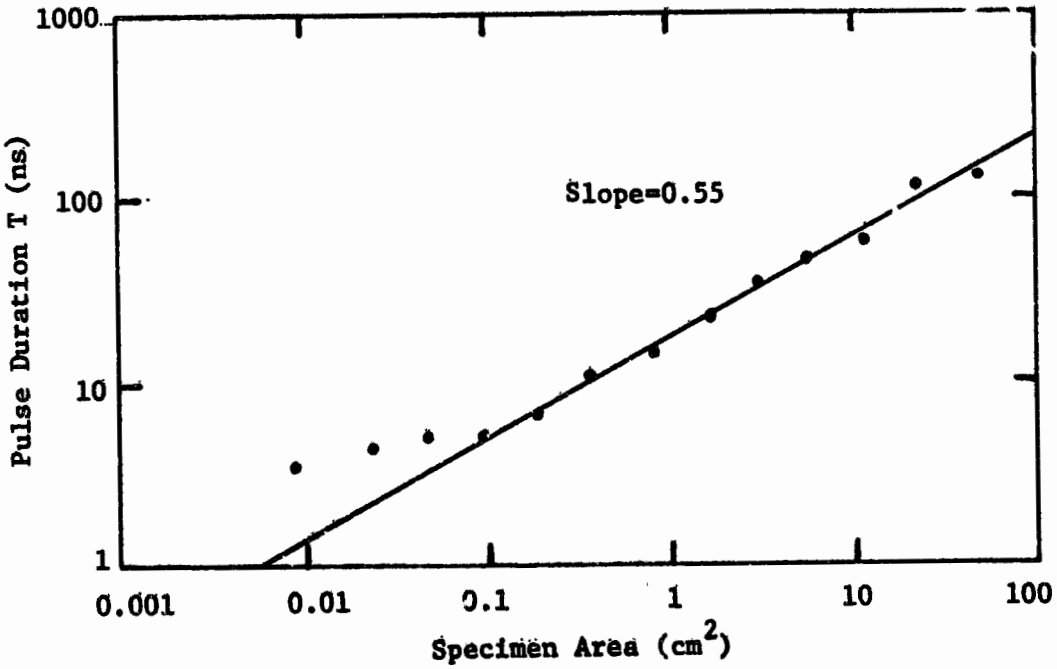

Figure 7. The variation of pulse duration $T = \frac{1}{I_m} \int I \, dt$ with Mylar specimen area.

Figure 8. Secondary electron image in a scanning electron microscope of a gold-coated, damaged Mylar specimen.

Figure 9. Transmitted-light microscope photograph of the specimen shown in Figure 8.

1 kV, 5 mm dia. 1 kV, 10 mm dia. 1 kV, 2.5 mm dia.

20 kV, 3 mm dia. 20 kV, 3 mm dia. 1 kV, 3 mm dia.

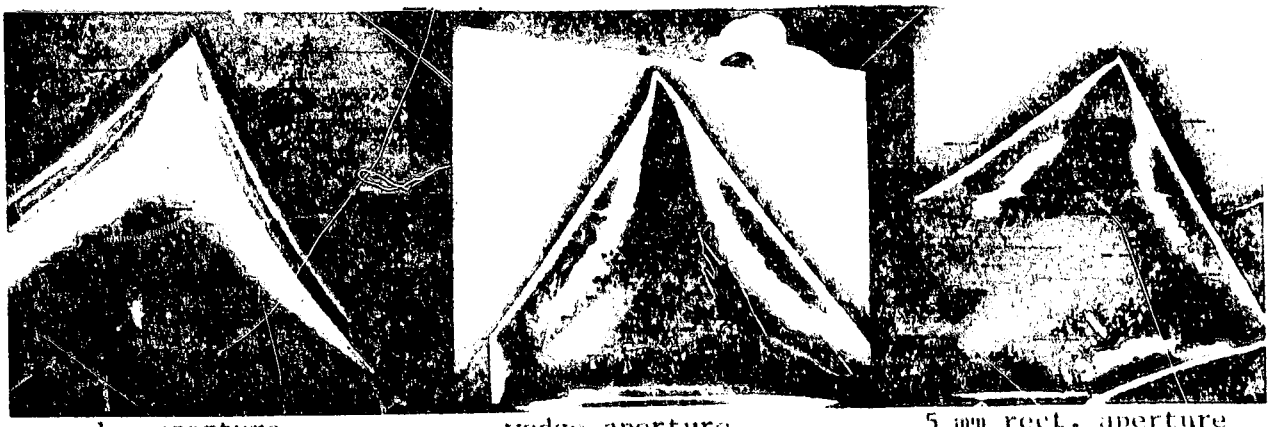

wedge aperture 20 kV

wedge aperture 1 kV

5 mm rect. aperture 1 kV

Figure 10. Charge accumulation on masked Teflon specimens as viewed by secondary-electron imaging in a scanning electron microscope (top right image is Mylar). All specimens have been charged by a 20 kV scanned beam. The apertures are in grounded aluminum metallization. The voltages given are those used for imaging.